Self-induced transparency and coherent population trapping of ^{87}Rb vapor in a mode-locked laser

Koji Masuda,[1] Christoph Affolderbach,[2] Gaetano Mileti,[2] Jean-Claude Diels,[1,*] and Ladan Arissian[1]

[1]*Center for High Technology Materials, University of New Mexico, Albuquerque, New Mexico 87106, USA*

[2]*Laboratoire Temps-Fréquence, University of Neuchâtel, Neuchâtel, Switzerland*

*Corresponding author: jcdiels@unm.edu

Simultaneous self-induced transparency and a dark line resonance are observed *inside* a mode-locked laser. The circulating pulse, tuned to the 795-nm optical resonance of rubidium, has sufficient intensity to create at each passage a population inversion—return to ground state, typical of self-induced transparency. A drop in fluorescence (dark line resonance), is observed as the repetition rate is tuned to a submultiple of the hyperfine ground-state splitting.

This work is part of a broader investigation into the complex properties of laser cavities to probe materials or fields inserted in them. For instance, in broad-band multimode lasers, a trace amount of intracavity substance with an absorption at ω_0 is sufficient to eliminate the adjacent modes [1]. If the modes are locked, the laser produces a frequency comb, of which the characteristics—repetition rate and carrier frequency to envelope offset (CEO)—are extremely sensitive to the dispersive properties of intracavity elements. This property was exploited to measure intracavity phase shifts of less than 10^{-8} [2]. Intracavity phase interferometry has been applied to magnetometry by inserting a transparent sample with nonzero Verdet constant in a ring laser with two-pulses per cavity roundtrip [3]. This intracavity technique can significantly enhance the sensitivity of an atomic magnetometer. Towards this goal, the present work explores the intracav-ity interaction of rubidium in a mode-locked laser.

The dispersion associated with the narrow resonances of alkali vapors can be manipulated via optical pumping [4] to produce large index of refraction without absorption, leading to coherent population trapping (CPT) [5] and electromagnetically induced transparency (EIT)[6,7]. The coherence is generally established by an exter-nal radio-frequency field, or by fine tuning of narrow-band "probe" and "pump" lasers as in Ref. [8]. In this approach, it has been shown that instantaneous phase shifts in the narrow band semiconductor lasers can destroy the ground-state coherence. The situation is different when the coherence is established by tuning the repetition rate of the pulses applied to the system. Computer simulation and extracavity experiments have demonstrated that the ground state coherence is not affected by instantaneous phase shifts in the radiation [9], contrary to the case treated by Abi-Salloum *et al.* [8]. In the case of *intracavity interaction*, the successive pulses are *in phase*, and such instantaneous phase shifts do not exist. Sub-kHz dark resonances were observed by tuning the repetition rate [9]. The experiments presented here demonstrate that coherent interaction can effectively be realized *inside* the cavity of a mode-locked laser.

Lasing builds up to a minimum loss configuration, which is why in a broadband multimode laser, the modes resonant with an absorption line are suppressed [1]. In a mode-locked laser tuned to the resonance of a narrow line absorber, several low-loss options are possible. In "zero-area pulse transmission" [10,11], each successive pulse has opposite phase, or, in frequency space, the atomic resonance is midway between two modes of the comb. Alternatively, each pulse of the train can have sufficient energy density to create a succession of population inversion—return to ground state. In that case, the energy lost to the medium in the first half of the pulse is restituted to the second half by stimulated emission. The condition is that the "pulse area" $\theta = \int_a^b \kappa \mathcal{E}(t) \mathrm{d}t > \pi$, where $\mathcal{E}$ is the electric field amplitude and $\kappa \mathcal{E}$ the Rabi frequency, and the integration limits $t = a, b$ refer to a time ahead and after an individual pulse. The energy density required to achieve the threshold $\theta = \pi$ being inversely proportional to the pulse duration, most experimental studies have been performed with ns pulses. The energy density of a picosecond pulse circulating inside the cavity of a mode-locked Ti:sapphire laser is sufficient to achieve $\theta \geq \pi$ for the $^5S_{1/2} \rightarrow {}^5P_{1/2}$ transition of ^{87}Rb. Lossless, distortionless, slow-light propagation of a resonant pulse, known as self-induced transparency [12] or SIT, occurs for an area ($\theta \approx 2\pi$) and shape $\kappa \mathcal{E} = (2/\tau_s)\mathrm{sech}(t/\tau_s)$ in a nondegenerate two-level system. The pulse duration (FWHM of the intensity) of this secant hyperbolic pulse is $\tau_p = 1.763\tau_s$.

Another aspect of the mode-locked laser that impacts the interaction with the atomic vapor is that the teeth of the comb are equally spaced [13,14]. Even though the modes of the laser cavity are not equally spaced, it has been shown [15] that the mode locking acts as an "orthodontic brace" to evenly space the teeth. The correction of the cavity dispersion occurs through the Kerr modulation [15]. A consequence of that property is that when multiple modes of the comb interact with ground-state atoms, the transition probability to the excited state vanishes, resulting in "coherent population trapping" (CPT) in the ground states. This coherent trapping oc-curs when the repetition rate of the laser (or the spacing

between tooth of the frequency comb) is equal to the hyperfine ground-state splitting of rubidium (or a submultiple thereof). The manifestation of CPT is observed as a reduction in fluorescence and absorption (a dark resonance), due to the reduced excited state population, and referred to as "dark line resonance" [5]. The dark line resonance observed by tuning the repetition rate of a mode-locked laser requires very low intensities, and therefore is not expected to be observed with the high-intensity pulse that circulates inside the mode-locked laser. It is shown here that despite the large intracavity intensities, coherent interaction makes possible the observation of a dark-line resonance induced by a frequency comb (CPT) *inside* a mode-locked laser resonator.

The physical situation leading to "self-induced transparency" is that of an inhomogeneously broadened 2-level system, which applies to ns pulses exciting Doppler broadened atomic vapor transitions. When the inhomogeneous linewidth is larger than the pulse bandwidth, an evolution law can be derived (the "area theorem" [12]) for the pulse area "θ":

$$\frac{d\theta_0}{dz} = -\frac{\alpha_0}{2} \sin\theta_0 , \qquad (1)$$

where α_0 is the linear absorption coefficient at the center of an *inhomogeneously broadened* nondegenerate two-level system. The solution $\theta(z)$ of Eq. (1) indicates that any pulse will evolve towards an area $2N\pi$ (N being an integer ≥ 0). The area $\theta_0 = 2\pi$ is a stable solution with the secant hyperbolic shape indicated before. For the 2π pulse, the leading edge loses its energy to the medium, which restitutes it to the trailing edge by stimulated emission, resulting in a pulse delay τ_d of one pulse duration per half absorption length or an envelope velocity $v_g = 2/(\alpha_0\tau_s)$ [12].

In contrast to the standard SIT situation, the present experiment involves picosecond pulses, much shorter than the inverse Doppler width of rubidium vapor ($1/T_2^* \approx 500$ MHz) they are interacting with. The area theorem does not apply in that case, but computer simulations have shown that coherent propagation effects do apply over propagation distances of the order of cT_2, where T_2 is the homogeneous linewidth [16]. Another complication is the level degeneracy, which implies a different Rabi coefficient κ_m for each (degenerate) sublevel m [17].

Our laser is a linear Ti:sapphire laser passively mode-locked by a multiple quantum well saturable absorber mirror (Fig. 1). The laser frequency is centered at 795 nm and fine tunable by a 3-plate birefringent filter. The repetition rate is adjustable by translating the output coupler. A vapor cell (6.5 cm long, 1.2 cm diameter with Brewster-angle windows) containing enriched ^{87}Rb (no buffer gas nor anti-relaxation coating are used) is placed near the output coupler. The cell assembly is composed of double-path heating wires for temperature control, temperature sensors, and one layer of μ-metal. A 3-mm-diameter hole on the side allows for fluorescence measurements. Mode-locked operation is achieved with the cell assembly inserted in the cavity. A beam is sent to an auto-correlator for pulse width measurements. With
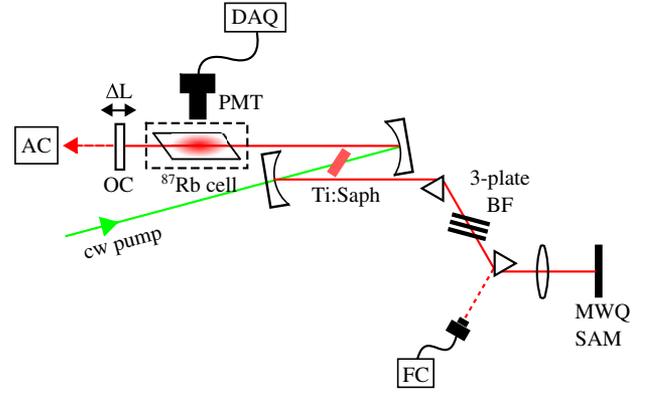

Fig. 1. Linear Ti:sapphire laser with an intracavity ^{87}Rb cell. Intracavity elements include multiple quantum well saturable absorber mirror (MQW-SAM), 3-plate birefringent filter (BF), output coupler (OC) on a translation stage, and the cell assembly (dashed box). The Pyrex cell has fused silica windows, which do not exhibit measurable birefringence. An output beam is sent to an auto-correlator (AC) for pulse width measurements. The repetition rate is monitored by a frequency counter (FC). The fluorescence is monitored by a photomultiplier tube (PMT).

the laser frequency tuned far off-resonance, a mode-locked pulse train of 6-ps pulses at 126.6492 MHz is generated [Figs. 2(a) and 2(b)]. Since the laser is not actively stabilized, the repetition rate fluctuates roughly over 10 Hz during a one minute measurement.

As the laser is tuned to resonance by adjusting the birefringent filter, a strong fluorescence signal is detected. A seven-fold pulse broadening is observed [Fig. 2(c)], and the repetition rate is reduced by 4 kHz, with fluctuations up to 200 Hz over one-minute measurement [Fig. 2(d)]. Pulse broadening and delay are typical results of reshaping effects as a pulse area increases with propagation towards the 2π value of self-induced transparency. The delay in the 2π pulse formation stage is very dependent
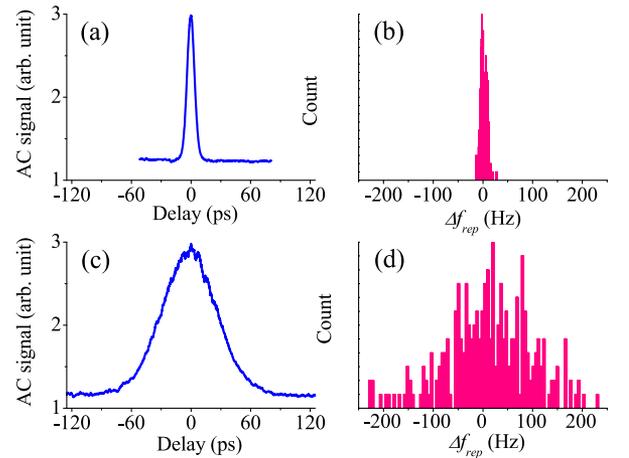

Fig. 2. Auto-correlation of the output pulse train and histogram of the laser repetition rate. (a) and (b) show an auto-correlation and the repetition rate fluctuations with the laser tuned far off resonance. As the laser tuned to the resonance, (c) significant shows pulse broadening, and (d) shows the enhanced fluctuations in repetition rate. The zero of the repetition rate scale in (d) is 4 kHz less than that of (b).

on the initial pulse area or intensity. Therefore, the intensity fluctuations manifest themselves as increased fluctuations of the repetition rate.

As the laser pump power is increased, successive lobes are seen to develop in the interferometric autocorrelations [18] of the pulses, indicating that the additional energy is transferred to lobes of opposite phase (an additional lobe for each 0.5 W of increase in pump power). The additional contribution of reversing electric field envelope is typical of "zero-area" pulse generation, as has been observed and predicted in absorbers [10,11] and amplifiers [19]. The additional zero-area lobes that cannot be resolved with a fast detector make an experimental determination of the pulse area difficult. The rough estimate below indicates that indeed, the intracavity pulse area is close to 2π. For an intracavity power $P = 4$ W, a cavity round-trip time $\tau_{rt} = 7.9$ ns, a pulse width $\tau_p = 63$ ps, and a beam diameter of $D = 0.8$ mm, $\theta \gtrsim 4\pi$ is obtained, As expected, this is an overestimate, because the energy used in the calculation includes a contribution that has a zero area (but not zero energy).

The above observations suggest that the threshold of coherent propagation has been reached. Effects of coherent propagation, such as group delay, scale with the linear absorption length. A measurement of the group delay as a function of the vapor number density indicates that coherent interaction is indeed at work and distinct from incoherent effects such as saturation. Measurements are performed for cell temperatures ranging from 22° to 70°. Group delays are deduced from the repetition rate and length of the cell. Experimental results plotted in Fig. 3 indicate a linear dependence of the envelope delay on the number density, which is expected if the delay is associated with the linear absorption coefficient.

To make a comparison with theory, we numerically integrate the Maxwell–Bloch equations for an inhomogeneously broadened medium using the Butcher predictor–corrector method. The rubidium vapor is approximated as a 3-level system consisting of two hyperfine ground-states, $|F = 1\rangle$ and $|F = 2\rangle$, and a single excited state with unresolved hyperfine states. In the slowly varying
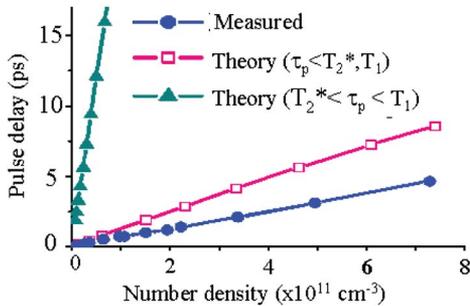

Fig. 3. Group delay as a function of the vapor number density. Experimental (blue-circle) data show a linear relation between the two. Numerical data (red-square) as a solution of (2)–(3). The green curve (triangles) shows the delay of one pulsewidth per half absorption length in the narrow-line limit $(T_2^* < \tau_p < T_1)$. The vapor pressure values are taken from the pressure/temperature tables from Ref. [20]. The temperature measurements made with a thermocouple placed between the heater and the cold finger of the cell may give an overestimate of the vapor pressure.

envelope approximation (SVEA) and after a transformation into a retarded frame, the Maxwell wave equation is reduced to

$$\frac{\partial \mathcal{E}}{\partial z} = -i \frac{\mu_0 \omega_\ell c}{2n} \bar{N} \int_0^\infty g(\omega_{ih})(\rho_{13}p_{13} + \rho_{23}p_{23})\mathrm{d}\omega_{ih}, \quad (2)$$

where $\mathcal{E}$ is a slowly varying envelope, ω_ℓ is the center angular frequency of the field, c is the speed of light, n is the refractive index of air, $\bar{N}$ is the number density of the ^{87}Rb vapor, $g(\omega_{ih})$ is inhomogeneous lineshape function, ρ_{ij} are the density matrix elements, and p_{ij} are the dipole moments. $g(\omega_{ih})$ is the 500-MHz Doppler broadening distribution. The time evolution of the density matrix elements is found by solving the interaction equations:

$$\frac{d\rho_{11}}{dt} = -\frac{\kappa}{2}\operatorname{Im}(\tilde{\mathcal{E}}^*\tilde{\sigma}_{31}) + \frac{\Gamma_3}{2}\rho_{33}$$

$$\frac{d\rho_{22}}{dt} = -\frac{\kappa}{2}\operatorname{Im}(\tilde{\mathcal{E}}^*\tilde{\sigma}_{32}) + \frac{\Gamma_3}{2}\rho_{33}$$

$$\frac{d\rho_{33}}{dt} = \frac{\kappa}{2}\operatorname{Im}(\tilde{\mathcal{E}}^*\tilde{\sigma}_{31}) + \frac{\kappa}{2}\operatorname{Im}(\tilde{\mathcal{E}}^*\tilde{\sigma}_{32}) - \Gamma_3\rho_{33}$$

$$\frac{d\tilde{\sigma}_{31}}{dt} = (-\Gamma_{31} - i\Delta_{13})\tilde{\sigma}_{31} - i\kappa\tilde{\mathcal{E}}(\rho_{33} - \rho_{11}) + i\kappa\tilde{\mathcal{E}}\tilde{\rho}_{21}$$

$$\frac{d\tilde{\sigma}_{32}}{dt} = (-\Gamma_{32} - i\Delta_{23})\tilde{\sigma}_{32} - i\kappa\tilde{\mathcal{E}}(\rho_{33} - \rho_{22}) + i\kappa\tilde{\mathcal{E}}\tilde{\rho}_{21}^*$$

$$\frac{d\tilde{\rho}_{21}}{dt} = (-\Gamma_{21} - i\Delta_{12})\tilde{\rho}_{21} - i\frac{\kappa}{4}\tilde{\mathcal{E}}^*\sigma_{31} - i\frac{\kappa}{4}\tilde{\mathcal{E}}\tilde{\sigma}_{32}^*, \quad (3)$$

where $\kappa = p/\hbar$ with $p_{ij} = p = 2.536 \times 10^{-29}$ Cm for the D1 transition, $\Delta_{ij} = \omega_\ell - \omega_{ij}$ represent a detuning from ij-transition, Γ_i are energy relaxation rates, and Γ_{ij} are phase relaxation rate. The relaxations are $\Gamma_3 = 2\pi \times 1/27.7$ ns, $\Gamma_{31,32} = \Gamma_3/2$, $\Gamma_{21} = 2\pi \times 300$ kHz is the transit time broadening. For the numerical simulation, we choose the light frequency midway between the hyperfine split levels (splitting f_{hs}) such that $\Delta_{13} = -\Delta_{23} = 2\pi f_{hs}$. The propagation of a 2π pulse of duration $\tau_p = 25$ ps is simulated.

Integration of (2) is executed over $z = 13.0$ cm, twice the length of the vapor cell to account for the second path through the cell after reflection off the output coupler. The envelope delay is measured by displacement of the peak of an output pulse with respect to the input pulse. A result of the numerical simulation is overlaid in Figure 3. Linear dependence of group delay on the number density is also revealed. The larger theoretical group delay may be attributed to an overestimate of the temperature of the rubidium, which was measured between the heater and the glass of the cold finger. Gain dynamics is another factor that affects the group delay, a property that is exploited to tune the repetition rate of frequency combs [21]. This gain acceleration however is orders of magnitude smaller than the group velocity changes that we are experiencing. Other slow-light effects resulting from large resonant dispersion in atomic vapors [22] do not apply for ultrashort pulses, since they are limited to a spectral region that is orders of magnitude smaller than the ps pulse bandwidth.
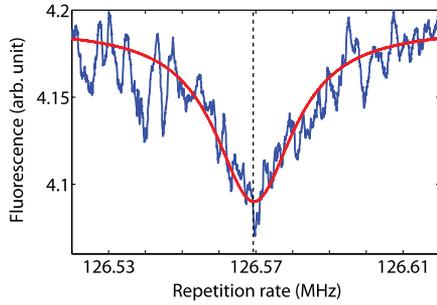
Fig. 4. Fluorescence signal as a function of the laser repetition rate. A reduction of fluorescence is seen at 126.568 MHz, 54th subharmonic of the ground state hyperfine splitting. The dashed line is a Lorentzian fit with a FWHM of 13 kHz.

Next, we experimentally investigate a possibility of CPT inside a mode-locked laser by tuning the repetition rate to an integer subharmonic (54th) of the ground-state hyper-fine splitting [9]. Figure 4 shows the dark line feature in the fluorescence signal collected from the vapor cell. The appearance of a dark-resonance is consistent with the previous experiment performed outside a cavity, and is a clear evidence of CPT. The physical linewidth of the dark resonance of 700 kHz (54 × 13 kHz) is larger than the minimum linewidth predicted from the time of flight through the beam, partly because of imperfect magnetic field shielding and partly due to optical power broadening, consistent with previous extracavity experiment [9].

In conclusion, we have experimentally investigated the interaction of rubidium vapor with picosecond mode-locked pulses inside a mode-locked laser cavity. Large pulse area inside the cavity makes coherent slow-light propagation to occur. Observations of pulse-broadening, slow-light, large pulse area ($\theta > 2\pi$) inside the cavity, strong dependence of group delay on the vapor number density, together with a numerical simulation of the Maxwell–Bloch equation, are consistent with character-istics of self-induced transparency. Furthermore, we have employed the repetition rate spectroscopy to inves-tigate CPT in the laser cavity. A narrow dark resonance is observed at the resonant repetition rate. Potential appli-cations include the realization of autostabilized all-optical frequency standards [9] and atomic intracavity phase interferometry (IPI) magnetometry [3].

References

1. T. W. Hänsch, A. L. Schawlow, and P. E. Toschek, IEEE J. Quantum Electron. **8**, 802 (1972).
2. L. Arissian and J.-C. Diels, Laser Photon. Rev. **8**, 799 (2014).
3. A. Schmitt-Sody, K. Masuda, A. Velten, L. Arissian, and J.-C. Diels, "Optical magnetic field detection by intracavity phase interferometry," in *17th International Conference on Ultrafast Phenomena (UP 2010)*, Snowmass, Colorado (2010), p. 39.
4. W. Happer, Rev. Mod. Phys. **44**, 169 (1972).
5. E. Arimondo, Phys. Rev. A **54**, 2216 (1996).
6. M. Fleischhauer, C. Keitel, M. Scully, C. Su, B. T. Ulrich, and S.-Y. Zhu, Phys. Rev. A **46**, 1468 (1992).
7. M. Fleischhauer, A. Imamoglu, and J. Marangos, Rev. Mod. Phys. **77**, 633 (2005).
8. T. Abi-Salloum, J. P. Davis, C. Lehman, E. Elliott, and F. A. Narducci, J. Mod. Opt. **54**, 2459 (2007).
9. L. Arissian and J.-C. Diels, Opt. Commun. **264**, 169 (2006).
10. H. P. Grieneisen, J. Goldhar, N. A. Kurnit, A. Javan, and H. R. Schlossberg, Appl. Phys. Lett. **21**, 559 (1972).
11. J.-C. Diels and E. L. Hahn, Phys. Rev. A **10**, 2501 (1974).
12. S. McCall and E. L. Hahn, Phys. Rev. **183**, 457 (1969).
13. T. Udem, J. Reichert, R. Holzwarth, and T. Hänsch, Opt. Lett. **24**, 881 (1999).
14. R. J. Jones, J. C. Diels, J. Jasapara, and W. Rudolph, Opt. Commun. **175**, 409 (2000).
15. L. Arissian and J.-C. Diels, J. Phys. B **42**, 183001 (2009).
16. T. Pierce and E. L. Hahn, "Self-induced-transparency in homogeneously broadened media," in *Bull. Am. Soc.; Annual Meeting of the Am. Phys. Soc.*, San Francisco (1972).
17. C. K. Rhodes, A. Szoke, and A. Javan, Phys. Rev. Lett. **21**, 1151 (1968).
18. J.-C. Diels, E. V. Stryland, and D. Gold, "Investigation of the parameters affecting subpicosecond pulse durations in pas-sively mode-locked dye lasers," in *Proceedings of the first Conference on Picosecond Phenomena*, Hilton Head, South Carolina (1978), pp. 117–120.
19. J.-C. Diels, Phys. Lett. A **31**, 26 (1970).
20. D. A. Steck, "Rubidium 87 d line data," available on line at http://steck.us/alkalidata (revision 2.1.1) (2009).
21. K. W. Holman, R. J. Jones, A. Marian, S. T. Cundiff, and J. Ye, Opt. Lett. **28**, 851 (2003).
22. R. M. Camacho, M. V. Pack, J. C. Howell, A. Schweinsberg, and R. W. Boyd, Phys. Rev. Lett. **98**, 153601 (2007).